

All-dielectric nanoantennas

Alexander E. Krasnok^a, Andrey E. Miroschnichenko^b, Pavel A. Belov^a, and Yuri S. Kivshar^{a,b}

^aNational Research University of Information Technologies,
Mechanics and Optics, St. Petersburg 197101, Russia

^bNonlinear Physics Centre, Research School of Physics and Engineering,
Australian National University, Canberra ACT 0200, Australia

ABSTRACT

The study of optical nanoantennas is a rapidly developing area of optics and nanophotonics. Nowadays, the most popular type of nanoantennas is a plasmonic one made of metallic elements. However, plasmonic nanoantennas have large dissipative losses. Here we present an overview of the recent results of a newly emerged field of *all-dielectric* optical nanoantennas. These optical nanoantennas are made of high-permittivity low-loss dielectric particles. Moreover, in addition to the electric resonances such nanoscale particles exhibit very strong magnetic response in the visible range. We introduce and study a highly efficient Huygens element and Yagi-Uda type nanoantennas based on dielectric nanoparticles. We also introduce a novel concept of all-dielectric superdirective nanoantennas based on the generation of higher-order optically-induced magnetic multipole modes. For such superdirective dielectric nanoantennas, we predict the effect of beam steering at the nanoscale characterized by a subwavelength sensitivity of the beam radiation direction to the source position. Based on all these new properties, optical nanoantennas offer unique opportunities for applications such as optical communications, photovoltaics, non-classical light emission, and sensing.

Keywords: Nanophotonics, nanoantenna, Yagi-Uda nanoantenna, dielectric, superdirectivity

1. INTRODUCTION

The recently emerged field of optical nanoantennas is promising for its potential applications in various areas of nanotechnology. The ability to redirect propagating radiation and transfer it into localized subwavelength modes at the nanoscale^{1–8} makes the optical nanoantennas highly desirable for many applications. Originally, antennas were suggested as sources of electromagnetic radiation at radio frequencies and microwaves, emitting radiation via oscillating currents. Different types of antennas were suggested and demonstrated for the effective manipulation of the electromagnetic radiation.⁹ Conventional antennas provide a source of electromagnetic radiation, with their sizes being comparable with the operational wavelength. Recent success in the fabrication of nanoscale elements allows to bring the concept of the radio-frequency antennas to optics, leading to the development of *optical nanoantennas* consisting of subwavelength elements.⁶

Nowadays, the most famous nanoantennas are plasmonic nanoantennas which consist of an array of metallic, (usually silver or gold), nanoparticles and utilise the optical properties of plasmon resonances. Despite of a series of advantages of plasmonic nanoantennas associated with their small size and strong localization of the electric field, such nanoantennas have large dissipative losses resulting in low radiation efficiency. In addition, the transmission type of plasmonic nanoantenna located on a substrate direct light mostly into the substrate, reducing their useful functionalities. In particular, these disadvantages hinder the development of optical wireless communication^{10–12} on a chip.

To overcome these limitations, we propose a new type of nanoantenna based on dielectric nanoparticles with a high index dielectric constant. This type of nanoantennas has several unique features such as low optical losses at the nanoscale and superdirectivity. The concept of all-dielectric nanoantennas has been developed in our original papers^{13–16} and also summarized below.

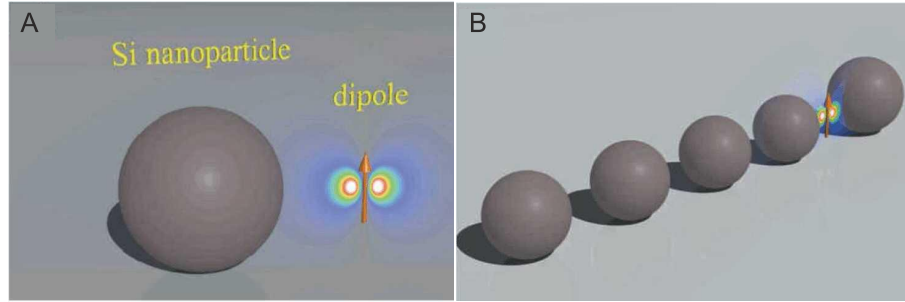


Figure 1. (A) Huygens element consisting of a single silicon nanoparticle and point-like dipole source separated by a distance $G_{ds} = 90$ nm (between dipole and sphere surface). The radius of the silicon nanoparticle is $R_s = 70$ nm. (B) Dielectric optical Yagi-Uda nanoantenna, consisting of the reflector of the radius $R_r = 75$ nm, and smaller director of the radii $R_d = 70$ nm. The dipole source is placed equally from the reflector and the first director surfaces at the distance G . The separation between surfaces of the neighbouring directors is also equal to G .

2. HUYGENS SOURCE AND DIELECTRIC YAGI-UDA NANOANTENNA

Recently, it was suggested^{13–15} a novel type of optical nanoantennas made of all-dielectric elements. Moreover, we argue that, since the source of electromagnetic radiation is applied externally, dielectric nanoantennas can be considered as the best alternative to their metallic counterparts. First, dielectric materials exhibit low loss at the optical frequencies. Second, as was suggested earlier,¹⁷ nanoparticles made of high-permittivity dielectrics may support both electric and magnetic resonant modes. This feature may greatly expand the applicability of optical nanoantennas for, e.g. detection of magnetic dipole transitions of molecules. In our study we concentrate on nanoparticles made of silicon. The real part of the permittivity of the silicon is about 16,¹⁸ while the imaginary part is up to two orders of magnitude smaller than that of noble metals (silver and gold).

2.1 General concept

The above mentioned properties of all-dielectric nanoparticles allow us to realize an optical Huygens source⁹ consisting of a point-like electric dipole operating at the magnetic resonance of a dielectric nanosphere (Fig.1A). Such a structure exhibits high directivity with vanishing backward scattering and polarization independence, being attractive for efficient and compact designs of optical nanoantennas.

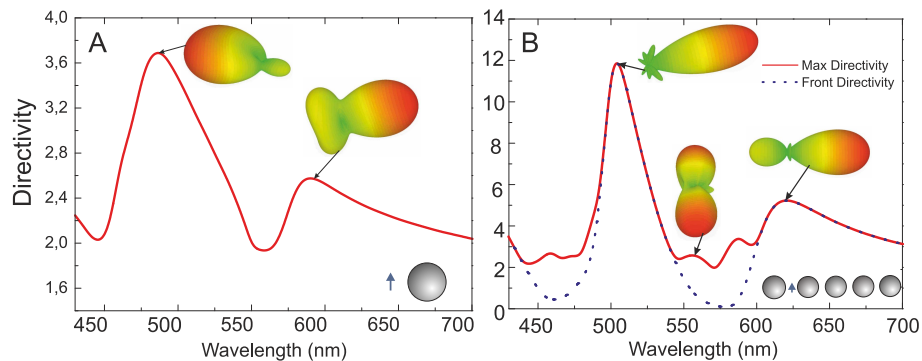


Figure 2. (A) Dependence of the directivity D on the wavelength. (B) Directivity of the dielectric Yagi-Uda nanoantenna vs wavelength for the separation distance $G = 70$ nm. Insert demonstrates 3D radiation pattern diagrams at particular wavelengths.

In Fig. 2A we show the dependence of the Directivity on wavelength for a single dielectric nanoparticle excited by a electric dipole source. Two inserts demonstrate 3D angular distribution of the radiated pattern $p(\theta, \varphi)$ corresponding to the local maxima. In this case, the system radiates predominantly to the forward direction at $\lambda = 590$ nm, while at $\lambda = 480$ nm, the radiation is predominantly in the backward direction. In this case, the total electric dipole moment of the sphere and point-like source and the magnetic dipole moment of the

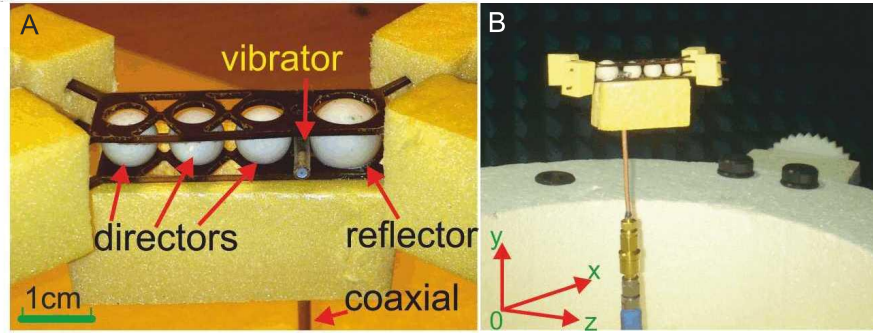


Figure 3. Photographs of the all-dielectric Yagi-Uda microwave antenna. (A) Detailed view of the antenna placed in a holder. (B) Antenna placed in an anechoic chamber; the coordinate z is directed along the vibrator axis; the coordinate y is directed along the antenna axis.

sphere oscillate with the phase difference $\arg(\alpha^m) - \arg(\alpha^e) = 1.3$ rad, resulting in the destructive interference in the forward direction. At the wavelength $\lambda = 590$ nm the total electric and magnetic dipole moments oscillate in phase and produce Huygens-source-like radiation pattern with the main lobe directed in the forward direction.

By adding more elements to the silicon nanoparticle, we can enhance the performance of all-dielectric nanoantennas. In particular, we consider a dielectric analogue of the Yagi-Uda design (see Fig.1) consisting of four directors and one reflector. The radii of the directors and the reflector are chosen to achieve the maximal constructive interference in the forward direction along the array. The optimal performance of the Yagi-Uda nanoantenna should be expected when the radii of the directors correspond to the magnetic resonance, and the radius of the reflector correspond to the electric resonance at a given frequency, with the coupling between the elements is taken into account. Our particular design consists of the directors with radii $R_d = 70$ nm and the reflector with the radius $R_r = 75$ nm. In Fig. 2B we plot the directivity of all-dielectric Yagi-Uda nanoantenna vs. wavelength with the separation distance $D = 70$ nm. Inserts demonstrate the 3D radiation patterns at particular wavelengths. We achieve a strong maximum at $\lambda = 500$ nm. The main lobe is extremely narrow with the beam-width about 40° and negligible backscattering. The maximum does not correspond exactly to either magnetic or electric resonances of a single dielectric sphere, which implies the importance of the interaction between constitutive nanoparticles.

2.2 Experimental verification of dielectric Yagi-Uda nanoantenna

To experimentally verify the concept of all-dielectric nanoantennas we use the scalability of the Maxwell's equations up to microwaves. Figures 3A,B show the photographs of the fabricated all-dielectric Yagi-Uda antenna.

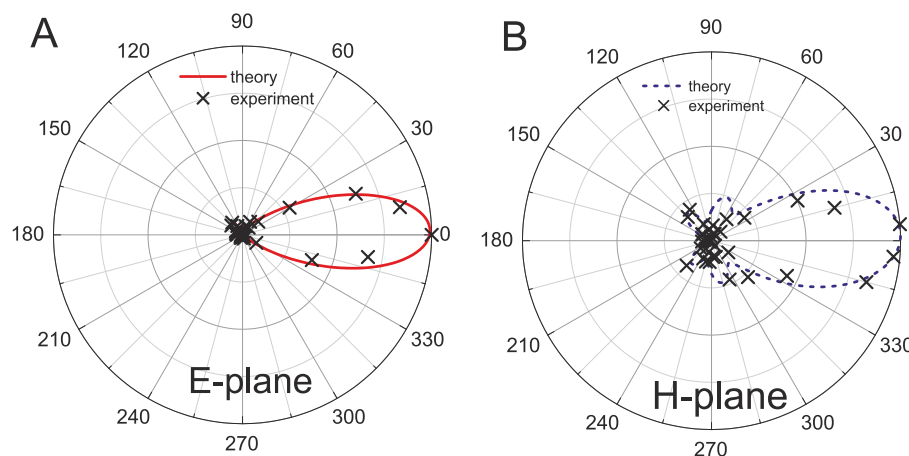


Figure 4. Radiation pattern of the antenna in (A) E -plane and (B) H -plane at the frequency 10.7 GHz. Solid lines show the results of numerical simulations in CST; the crosses correspond to the experimental data.

To mimic the silicon spheres at the microwave frequency range, we employ MgO-TiO₂ ceramic which is characterized by dielectric constant of 16 and dielectric loss factor of $(1.12-1.17)10^{-4}$ measured at 9-12 GHz frequency range. As a source, we use a half-wavelength vibrator. We study experimentally both the radiation pattern and directivity of the antenna.

The antenna radiation patterns in the far field (at the distance $\simeq 3$ m, $\simeq 100\lambda$) are measured in an anechoic chamber by a horn antenna and rotating table. The measured radiation patterns of the antenna in *E*- and *H*-planes at the frequency 10.7 GHz are shown in Fig. 4. The measured characteristics agree very well with the numerical results.

3. SUPERDIRECTIVE DIELECTRIC OPTICAL NANOANTENNAS

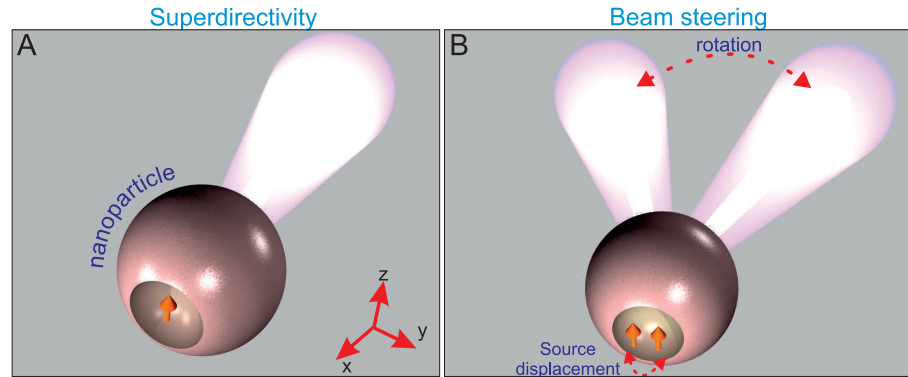


Figure 5. (A) Geometry of an all-dielectric superdirective nanoantenna excited by a point-like dipole. (B) Concept of the beam steering effect at the nanoscale.

For optical wireless circuits on a chip, nanoantennas are required to be both highly directive and compact.¹⁰⁻¹² In nanophotonics, directivity has been achieved for arrayed plasmonic antennas utilizing the Yagi-Uda design,^{6, 11, 15, 19, 20} large dielectric spheres,²¹ and metascreen antennas.²² Though individual elements of these arrays are optically small, the overall size of the radiating systems is larger than the radiation wavelength λ . In addition, small plasmonic nanoantennas possess weak directivity close to the directivity of a point dipole.²³⁻²⁵

Recently, it was suggested theoretically and experimentally to employ magnetic resonances of high-index dielectric nanoparticles for enhancing the nanoantenna directivity.^{14, 15, 26} High-permittivity nanoparticles can have nearly resonant balanced electric and magnetic dipole responses.^{13, 15, 26-29} This balance of the electric and magnetic dipoles oscillating with the same phase allows the practical realization of the Huygens source, an elementary emitting system with a cardioid pattern^{9, 13-15} and with the directivity larger than 3.5. Importantly, a possibility to excite magnetic resonances leads to the improved nanoantenna directional properties without a significant increase of its size.

Superdirectivity has been already discussed for radio-frequency antennas, and it is defined as directivity of an electrically small radiating system that significantly exceeds (at least in 3 times) directivity of an electric dipole.^{9, 30, 31} In that sense, the Huygens source is not superdirective. In the antenna literature, superdirectivity is claimed to be achievable only in antenna arrays by the price of ultimately narrow frequency range and by employing very precise phase shifters (see, e.g., Ref.^{9, 30, 31}). Therefore, superdirective antennas, though very desirable for many applications such as space communications and radioastronomy, were never demonstrated and implemented for practical applications.

Superdirectivity was predicted theoretically for an antenna system²² where some phase shifts were required between radiating elements to achieve complex shapes of the elements of a radiating system which operates as an antenna array. In this paper, we employ the properties of subwavelength particles excited by an inhomogeneous field with higher-order magnetic multipoles. We consider a subwavelength dielectric nanoantenna (with the size of 0.4λ) with a notch resonator excited by a point-like emitter located in the notch. The notch transforms the energy of the generated magnetic dipole Mie-type resonance into high-order multipole moments, where the

magnetic multipoles dominate. This system scatters light resonantly, i.e. it is very different from dielectric lenses and usual dielectric cavities which are large compared to the wavelength. Another important feature of the notched resonator is huge sensitivity of the radiation direction to a spatial position of the emitter. This property leads to a strong beam steering effect and subwavelength sensitivity of the radiation direction to the source location. The proposed design of superdirective nanoantennas may also be useful for collecting single-source radiation, monitoring quantum objects states, and nanoscale microscopy.

In order to achieve superdirectivity, we should generate subwavelength spatial oscillations of the radiating currents.^{9,30,31} Then, near fields of the antenna become strongly inhomogeneous, and the near-field zone expands farther than that of a point dipole. This results in a growth of the effective antenna aperture which is associated with the maximum of directivity $D_{\max} = 4\pi P_{\max}/P_{\text{tot}}$, being defined as $S = D_{\max}\lambda^2/(4\pi)$, where λ is the wavelength of radiation in free space, P_{\max} and P_{tot} are the maximum power in the direction of the radiation pattern and the total radiation power, respectively. Normalizing the effective aperture S by the geometric aperture for a spherical antenna $S_0 = \pi R_S^2$, we obtain the definition of superdirectivity in the following form:^{9,30}

$$S_n = \frac{D_{\max}\lambda^2}{4\pi^2 R_S^2} \gg 1$$

Practically, the value $S_n = 4 \dots 5$ is sufficient for superdirectivity of a sphere. In this work, maximum of 6.5 for S_n is predicted theoretically for the optical frequency range, and the value of 5.9 is demonstrated experimentally for the microwave frequency range.

3.1 Concept of superdirective dielectric nanoantennas

Here we demonstrate a possibility to create a superdirective nanoantenna without hypothetical metamaterials and plasmonic arrays. We consider a silicon nanoparticle, taking into account the frequency dispersion of the dielectric permittivity.¹⁸ The radius of the silicon sphere is equal in our example to $R_S = 90$ nm. For a simple sphere under rather homogeneous (e.g. plane-wave) excitation, only electric and magnetic dipoles can be resonantly excited while the contribution of higher-order multipoles is negligible.¹⁵ Making a notch in the sphere breaks the symmetry and increases the contribution of higher-order multipoles into scattering even if the sphere is still excited homogeneously. Further, placing a nanoemitter (e.g. a quantum dot) inside the notch, as shown in Fig. 5 we create the conditions for the resonant excitation of multipoles: the field exciting the resonator is now spatially highly non-uniform as well as the field of a set of multipoles. In principle, the notched particle operating as a nanoantenna can be performed of different semiconductor materials and have various shapes – spherical, ellipsoidal, cubic, conical, as well as the notch. However, in this work, the particle is a silicon sphere and the notch has the shape of a hemisphere with a radius $R_N < R_S$. The emitter is modeled as a point-like dipole and it is shown in Fig. 5 by a red arrow.

It is important to mention that our approach is seemingly close to the idea of Refs.^{32,33} where a small notch on a surface of a semiconductor microlaser was used to achieve higher emission directivity by modifying the field distribution inside the resonator.³⁴ An important difference between those earlier studies and our work is that the design discussed earlier is not optically small and the directive emission is not related to superdirectivity. In our case, the nanoparticle is much smaller than the wavelength, and our design allows superdirectivity. For the same reason our nanoantenna is not dielectric^{35,36} or Luneburg^{37,38} lenses. For example, immersion lenses^{39–42} are the smallest from known dielectric lenses, characterized by the large size 1-2 μm in optical frequency range. The functioning of such lenses is to collecting a radiation by large geometric aperture S , while $S_n \simeq 1$. Our approach demonstrates that the subwavelength system, with small geometric aperture, can have high directing power because of an increase of the effective aperture. Moreover, there are articles (see. Refs.^{43,44}) where the transition rates of atoms inside and outside big dielectric spheres with low dielectric constant (approximately 2), were studied.

First, we consider a particle without a notch but excited inhomogeneously by a point emitter. To study the problem numerically, we employed the simulation software CST Microwave Studio. Image Fig. 6A shows the dependence of the maximum directivity D_{\max} on the position of the source in the case of a sphere $R_S = 90$ nm without a notch, at the wavelength $\lambda = 455$ nm (blue curve with crosses). This dependence has the maximum ($D_{\max} = 7.1$) when the emitter is placed inside the particle at the distance 20 nm from its surface. The analysis

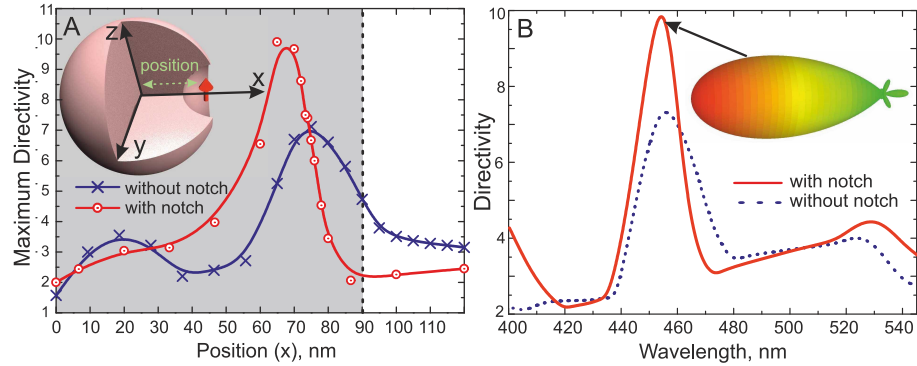


Figure 6. (A) Maximum of directivity depending on the position of the emitter ($\lambda = 455$ nm) in the case of a sphere with and without notch. Vertical dashed line marks the particle radius centered at the coordinate system. (B) Directivity dependence on the radiation wavelength. The inset shows three-dimensional radiation pattern of the structure ($R_S = 90$ nm and $R_N = 40$ nm).

shows that in this case the electric field distribution inside a particle corresponds to the noticeable excitation of higher-order multipole modes not achievable with the homogeneous excitation.

Furthermore, the amplitudes of high-order multipoles are significantly enhanced via making a small notch around the emitter. As it is shown in Fig. 5, this geometry transforms it into a resonator for high-order multipole moments. In this example the center of the notch is on the nanosphere's surface. The optimal radius of the notch (for maximal directivity) is equal $R_N = 40$ nm. In Fig. 6A the extrapolation red curve with circles, corresponding to simulation results, shows the maximal directivity versus the location of the emitter at the wavelength 455 nm. The maximal directivity $D_{\max} = 10$ is achieved at this wavelength as one can see from Fig. 6B that shows the directivity versus λ with and without a notch. The inset shows the three-dimensional radiation pattern of the structure at $\lambda = 455$ nm. This pattern has an angular width (at the level of 3 dB) of the main lobe equal to 40° . This value of directivity corresponds to the normalized effective aperture $S_n = 6.5$.

Figs. 7A,B show the distribution of the absolute values and phases of the internal electric field and this field in the vicinity of the nanoantenna. Electric field inside the particle is strongly inhomogeneous at $\lambda = 455$ nm i.e. in the regime of the maximal directivity (the same holds for the magnetic field, as shown in Fig. 7C,D). In this regime, the internal area where the electric field oscillates with approximately the same phase turns out to be maximal. This area is located near the back side of the spherical particle, as can be seen in Fig. 7B,D. In other words, the effective near zone of the nanoantenna in the superdirective regime of is maximal.

Usually, high directivity of plasmonic nanoantennas is achieved by excitation of higher *electrical* multipole moments in nanoparticles⁴⁵⁻⁴⁷ or for core-shell resonators consisting of a plasmonic material and a hypothetical metamaterial which would demonstrate the extreme material properties in the nanoscale.⁴⁸ Although, the values of directivity achieved for such nanoantennas do not allow superdirectivity, these studies stress the importance of higher multipoles for the antenna directivity.

We have performed the transformation of multipole coefficients into an angular distribution of radiation by using distribution of the electric and magnetic fields Fig.7A-D and determined the relative contribution of each order l . Fig. 7E shows how the directivity grows versus the spectrum of multipoles with equivalent amplitudes. The right panel of Fig. 7E nearly corresponds to the inset in Fig. 6 that fits to the results shown in Fig. 7E.

Generally, the superdirectivity effect has been accompanied by a significant increase of the effective near field zone of the antenna compared to that of a point dipole for which the near zone radius is equal $\lambda/2\pi$. In the optical frequency range this effect is especially important, considering the crucial role of the near fields at the nanoscale.

Usually, the superdirectivity regime corresponds to a strong increase of dissipative losses.⁹ Radiation efficiency of the nanoantenna is determined by $\eta_{\text{rad}} = P_{\text{rad}} / (P_{\text{rad}} + P_{\text{loss}})$, where P_{loss} is the power of losses in an nanoantenna. However, the multipole moments excited in our nanoantenna are mainly of magnetic type that leads to a strong increase of the near magnetic field that dominates over the electric one. Since the dielectric

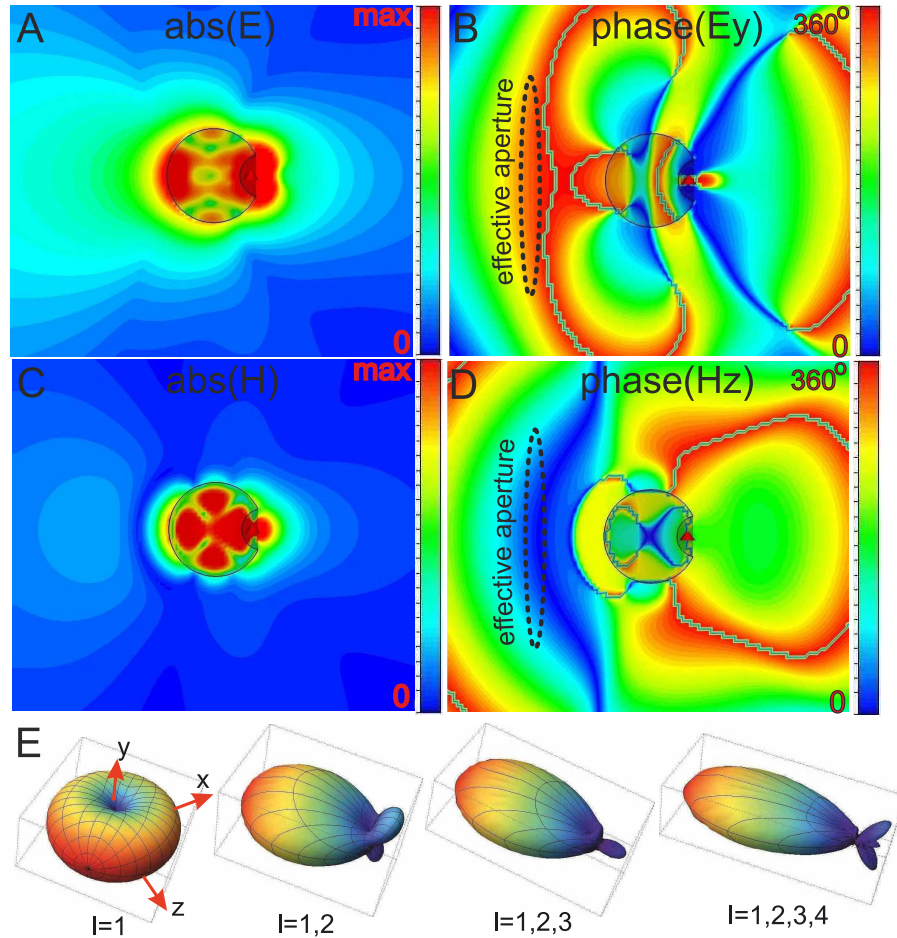


Figure 7. Distribution of (A) absolute values and (B) phases of the electric field (C and D for magnetic field, respectively) of the all-dielectric superdirective nanoantenna with source in the center of notch, at the wavelength $\lambda = 455$ nm. (E) Dependence of the radiation pattern of all-dielectric superdirective nanoantenna on the number of taken into account multipoles. Dipole like source located along the z axis.

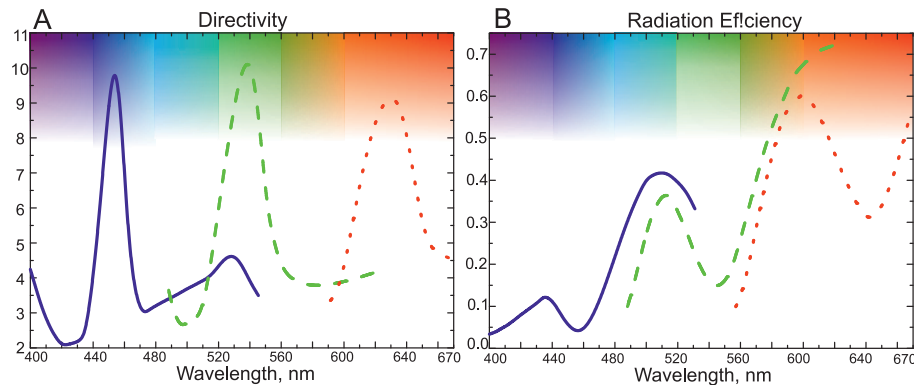


Figure 8. Dependence of directivity (A) and radiation efficiency (B) on the size of nanoantenna. Here, the blue solid lines corresponds to the geometry – $R_S = 90$ nm, $R_N = 40$ nm, the green dashed curves – $R_S = 120$ nm, $R_N = 55$ nm and red point curves – $R_S = 150$ nm, $R_N = 65$ nm. Growth of the nanoantenna efficiency due to the reduction of dissipative losses in silicon with increasing of wavelength.

material does not dissipate the magnetic energy, the effect of superdirectivity does not lead to a so large increase of losses in our nanoantenna as it would be in the case of dominating electric multipoles. However, since the electric

near field is nonzero the losses are not negligible. At wavelengths 440-460 nm (blue light) the directivity achieves 10 but the radiation efficiency is less than 0.1 (see Fig. 8). This is because silicon has very high losses in this range.¹⁸ Peak of directivity is shifted to longer wavelengths with increasing the size of the nanoantenna. For the design parameters corresponding to the operation wavelength 630 nm (red light) the calculated value of radiation efficiency is as high as 0.5, with nearly same directivity close to 10. In the infrared range, there are high dielectric permittivity materials with even lower losses. In principle, the proposed superdirectivity effect is not achieved by price of increased losses, and this is an important advantage compared to known superdirective radio-frequency antenna arrays⁹ and compared to their possible optical analogues – arrays of plasmonic nanoantennas.

Additional studies have shown that the presence of the SiO₂ substrate does not lead to a significant reduction of the directivity compared to the above results where the nanoantenna is located in free space. The absence of the impact of a dielectric substrate is explained by the magnetic nature of the nanoantenna operation.

3.2 Steering of light at the nanoscale

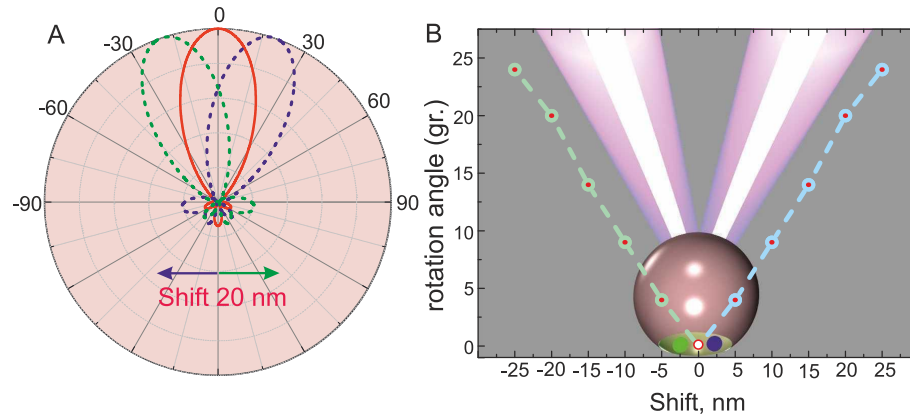


Figure 9. The rotation effect of the main beam radiation pattern, with subwavelength displacement of emitter inside the notch. (A) The radiation patterns of the antenna with the source in center (solid line) and the rotation of the beam radiation pattern for the 20 nm left/right offset (dashed lines). (B) Dependence of the the rotation angle on the source offset.

Here we examine the response of the nanoantenna to subwavelength displacements of the emitter. Displacement in the plane perpendicular to the axial symmetry of antenna (i.e. along the y axis) leads to rotation of the beam without damaging the superdirectivity. Image Fig.9A shows the radiation patterns of the antenna with the source at the center (solid line) and the rotation of the beam for the 20 nm left/right offset (dashed lines). Shifting of the source right side leads to rotation of pattern to the left, and vice versa. The angle of the beam rotation is equal to 20 degrees, that is essential and available to experimental observations. The result depends on the geometry of the notch. For a hemispherical notch, the dependence of the rotation angle on the displacement is presented in Fig.9B.

Instead of the movement of a single quantum dot one can use the emission of multiple quantum dots located near the edges of the notch. In this case, the dynamics of their spontaneous decay will be well displayed in the angular distribution of the radiation. This can be useful for quantum information processing and for biomedical applications.

Beam steering effect described above is similar to the effect of beam rotation in hyperlens,⁴⁹⁻⁵¹ where the displacement of a point-like source leads to a change of the angular distribution of the radiation power. However, in our case, the nanoantenna has subwavelength dimensions and therefore it can be neither classified as a hyperlens nor as a micro-spherical dielectric nanoscope,^{35,36} moreover it is not an analogue of solid immersion micro-lenses,³⁹⁻⁴² which are characterized by the size 1-5 μm in the same frequency range. These lens has a subwavelength resolving power due to the large geometric aperture but the value of normalized effective aperture is $S_n \simeq 1$. Our study demonstrates that the sub-wavelength system, with *small compared to the wavelength* geometric aperture can have both high directing and resolving power *because of a strong increase of the effective aperture compared to the geometrical one*.

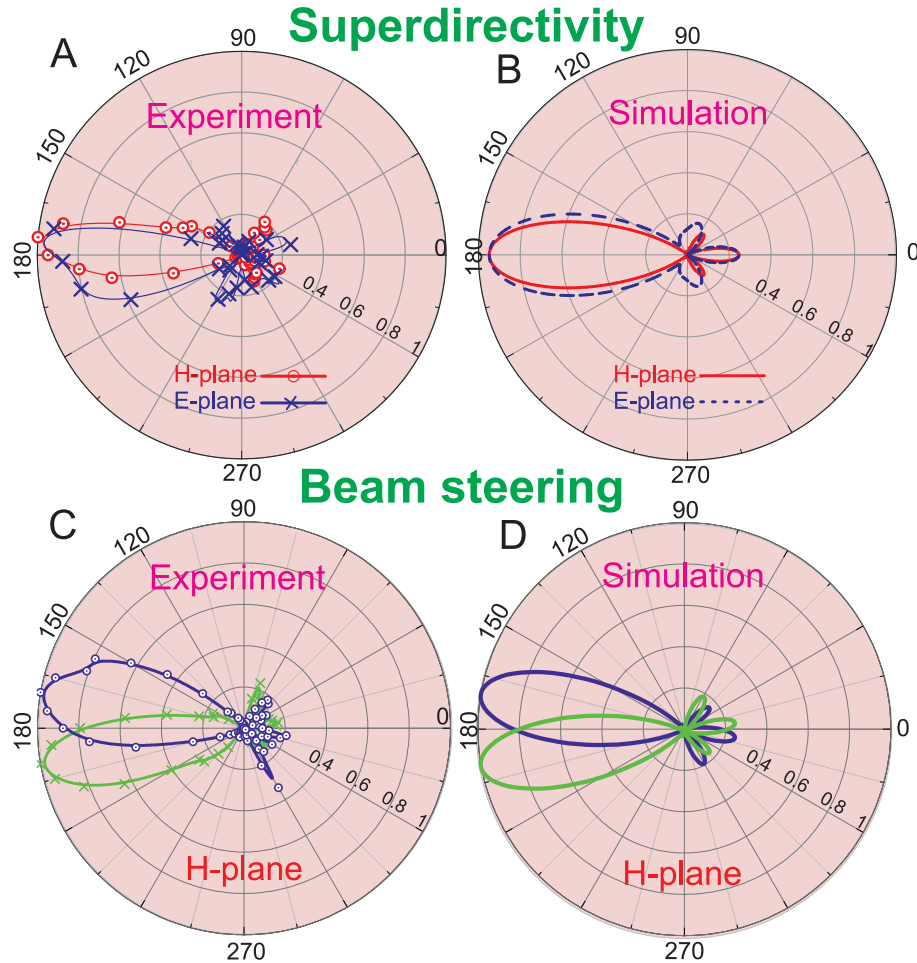


Figure 10. Experimental (A) and numerical (B) radiation patterns of the antenna in both E - and H -planes at the frequency 16.8 GHz. The crosses and circles correspond to the experimental data. Experimental (C) and numerical (D) demonstration of beam steering effect, displacement of dipole is equal 0.5 mm.

3.3 Experimental verification of superdirective dielectric nanoantennas

We have confirmed both predicted effects studying the similar problem for the microwave range. To do this, we have scaled up the nanoantenna as above to low frequencies. Instead of Si we employ MgO-TiO₂ ceramic¹⁴ characterized at microwaves by a dispersion-less dielectric constant 16 and dielectric loss factor of $1.12 \cdot 10^{-4}$. The results of the experimental investigations and numerical simulations of the pattern in both E - and H -planes are summarized in Figs. 10A,B. Radiation patterns in both planes are narrow beams with a lobe angle about 35°. Experimentally obtained coefficients of the directivity in both E - and H -planes are equal to 5.9 and 8.4, respectively (theoretical predictions for them were equal, respectively, 6.8 and 8.1). Our experimental data are in a good agreement with the numerical results except a small difference for the E plane, that can be explained by the imperfect symmetry of the emitter. Note, that the observed directivity is close to that of an all-dielectric Yagi-Uda antenna with overall size 2λ .¹⁴ The total size of our experimental antenna is closed to $\lambda/2.5$. Thus, our experiment clearly demonstrates the superdirective effect.

Experimental and numerical demonstration of the beam steering effect are presented in Figs. 10C,D. For the chosen geometry of antenna, displacement of source by 0.5 mm leads to a rotation of the beam about 10°. Note that the ratio of $\lambda = 18.7$ mm to value of the source displacement 0.5 mm is equal to 37. This proves that the beam steering effect observed at subwavelength displacement of source.

4. CONCLUSIONS

Here we have suggested and verified experimentally a new type of optical nanoantennas made of dielectric nanoparticles. Such all-dielectric nanoantennas demonstrate a number of key advantages over their metallic counterparts, including much lower dissipation losses and strong optically-induced magnetization. We have analyzed an all-dielectric analogue of the plasmonic Yagi-Uda nanoantenna consisting of an array of nanoelements, and have demonstrated very high directivity with a smaller number of directors. Moreover, lower dissipation losses and localization of the electromagnetic field inside the nanoparticles allows to reduce the distance between the adjacent elements even further, without compromising the performance. We have demonstrated experimentally that the microwave antennas composed of high-permittivity spheres provide the narrow radiation pattern of about 40° , as predicted by numerical calculations. This may allow to create a new generation of optical nanoantennas.

In addition, we have suggested a novel approach to achieve superdirectivity of antennas through the excitation of higher-order magnetic multipoles in an optically small dielectric nanoparticle with a notch and a point emitter located inside the notch. For the visible frequency range, we have studied this effect theoretically and demonstrated that a nanoemitter placed in the notch generates efficiently higher-order magnetic multipole modes responsible for a very high directivity of the nanoantenna not achievable by any other method. We have also suggested an efficient steering effect for an offset of the subwavelength source. We have demonstrated experimentally both superdirectivity and giant beam steering for the microwave frequency range. Combination of superdirectivity with the beam steering and the fact that both the effects can be observed for optical and microwave ranges makes our results very promising for numerous applications in radio physics and nanophotonics.

5. ACKNOWLEDGEMENTS

The authors thank B. Lukyanchuk, S. A. Tretyakov and V. V. Klimov for useful discussions and suggestions, and also E. A. Nenasheva and P. V. Kapitanova for a technical help. This work was supported by the Ministry of Education and Science of the Russian Federation (projects 11.G34.31.0020, 11.519.11.2037, 14.B37.21.0307, 14.132.21.1678, 01201259765), Dynasty Foundation (Russia), and the Australian Research Council.

REFERENCES

- [1] T. H. Taminiau, F. D. Stefani, and N. F. van Hulst, "Enhanced directional excitation and emission of single emitters by a nano-optical yagi-uda antenna.," *Opt. Express* **16**, pp. 16858–16866, 2008.
- [2] L. Novotny, "Optical antennas tuned to pitch," *Nature* **455**, p. 887, 2008.
- [3] A. F. Koenderink, "Plasmon nanoparticle array waveguides for single photon and single plasmon sources," *Nano Lett.* **9**, pp. 4228–4233, 2009.
- [4] T. Pakizeh and M. Kall, "Unidirectional ultracompact optical nanoantennas," *Nano Lett.* **9**, pp. 2343–2349, 2009.
- [5] A. Devilez, B. Stout, and N. Bonod, "Compact metallo-dielectric optical antenna for ultra directional and enhanced radiative emission," *ACS Nano* **4**, pp. 3390–3396, 2010.
- [6] L. Novotny and N. van Hulst, "Antennas for light," *Nat. Photon.* **5**, pp. 83–90, 2011.
- [7] J. Dorfmueller, D. Dregely, M. Esslinger, W. Khunsin, R. Vogelgesang, K. Kern, and H. Giessen, "Near-field dynamics of optical yagi-uda nanoantennas," *Nano Lett.* **11**, pp. 2819–2824, 2011.
- [8] A. E. Miroshnichenko, I. S. Maksymov, A. R. Davoyan, C. Simovski, P. Belov, and Y. S. Kivshar, "An arrayed nanoantenna for broadband light emission and detection," *Phys. Status Solidi RRL* **5**, pp. 347–349, 2011.
- [9] C. Balanis, *Antenna Theory: Analysis and Design*, New York ; Wiley, 1982.
- [10] A. Alu and N. Engheta, "Wireless at the nanoscale: Optical interconnects using matched nanoantennas," *Phys. Rev. Lett.* **104**, p. 213902, 2010.
- [11] P. Biagioni, J.-S. Huang, and B. Hecht, "Nanoantennas for visible and infrared radiation," *Rep. Prog. Phys.* **75**, p. 024402, 2012.
- [12] D. Solis, J. Taboada, F. Obelleiro, and L. Landesa, "Optimization of an optical wireless nanolink using directive nanoantennas," *Optics Express* **21**, p. 2369, 2013.
- [13] A. E. Krasnok, A. E. Miroshnichenko, P. A. Belov, and Y. S. Kivshar *JETP Lett.* **94**, p. 635, 2011.

- [14] D. S. Filonov, A. E. Krasnok, A. P. Slobozhanyuk, P. V. Kapitanova, E. A. Nenasheva, Y. S. Kivshar, and P. A. Belov, "Experimental verification of the concept of all-dielectric nanoantennas," *Appl. Phys. Lett.* **100**, p. 201113, 2012.
- [15] A. E. Krasnok, A. E. Miroshnichenko, P. A. Belov, and Y. S. Kivshar, "All-dielectric optical nanoantennas," *Optics Express* **20**, p. 20599, 2012.
- [16] A. Krasnok, D. Filonov, A. Slobozhanyuk, C. Simovski, P. Belov, and Y. Kivshar, "Superdirective dielectric nanoantennas with effect of light steering," *arxiv.org/abs/1307.4601*, 2013.
- [17] A. B. Evlyukhin, C. Reinhardt, A. Seidel, B. S. Lukyanchuk, and B. N. Chichkov, "Optical response features of si-nanoparticle arrays," *Phys. Rev. B* **82**, p. 045404, 2010.
- [18] E. Palik, *Handbook of Optical Constant of Solids*, San Diego, Academic, 1985.
- [19] D. Dregely, R. Taubert, J. Dorfmueller, R. Vogelgesang, K. Kern, and H. Giessen, "3d optical yagi-uda nanoantenna array," *Nat. Comm.* **2**, pp. 1-7, 2011.
- [20] Y. G. Liu, W. C. H. Choy, W. E. I. Sha, and W. C. Chew, "Unidirectional and wavelength-selective photonic sphere-array nanoantennas," *Optics Lett.* **37**, p. 2112, 2012.
- [21] A. Devilez, B. Stout, and N. Bonod, "Compact metallo-dielectric optical antenna for ultra directional and enhanced radiative emission," *ACS Nano* **4**, p. 3390, 2010.
- [22] A. Ludwig, C. Sarris, and G. Eleftheriades, "Metascreen-based superdirective antenna in the optical frequency regime," *Phys. Rev. Lett.* **109**, p. 223901, 2012.
- [23] P. K. Jain and M. A. El-Sayed, "Plasmonic coupling in noble metal nanostructures," *Chemical Physics Letters* **487**, 2010.
- [24] S. He, Y. Cui, Y. Ye, P. Zhang, and Y. Jin, "Optical nanoantennas and metamaterials," *Materials Today* **12**, p. 16, 2009.
- [25] S. R. K. Rodriguez, S. Murai, M. A. Verschuuren, and J. G. Rivas, "Light-emitting waveguide-plasmon polaritons," *Phys. Rev. Lett.* **109**, p. 166803, 2012.
- [26] B. N. Rolly B, Stout B, "Boosting the directivity of optical antennas with magnetic and electric dipolar resonant particles," *Optics Exp.* **20**, p. 20376, 2012.
- [27] A. B. Evlyukhin, S. M. Novikov, U. Zywiets, R. L. Eriksen, C. Reinhardt, S. I. Bozhevolnyi, and B. N. Chichkov, "Demonstration of magnetic dipole resonances of dielectric nanospheres in the visible region," *Nano Lett.* **12**, p. 3749, 2012.
- [28] A. I. Kuznetsov, A. E. Miroshnichenko, Y. H. Fu, J. Zhang, and B. Lukyanchuk, "Magnetic light," *Sci. Rep.* **2**, p. 492, 2012.
- [29] Y. Fu, A. Kuznetsov, A. Miroshnichenko, Y. Yu, and B. Lukyanchuk, "Directional visible light scattering by silicon nanoparticles," *Nat. Comm.* **4**, p. 1, 2013.
- [30] R. Hansen, *Electrically small, superdirective, and superconducting antennas*, Wiley-Interscience, 2006.
- [31] R. Hansen and R. Collin, *Small Antenna Handbook*, John Wiley and Sons Ltd, 2011.
- [32] S. Boriskina, T. Benson, P. Sewell, and A. Nosich, "Directional emission, increased free spectral range and mode q-factors in 2-d wavelength-scale optical microcavity structures," *IEEE J. Select. Topics Quantum Electron.* **12**, pp. 1175-1182, 2006.
- [33] Q. J. Wang, C. Yan, N. Yu, J. Unterhinninghofen, J. Wiersig, C. Pflugl, L. Diehl, T. Edamura, M. Yamashita, H. Kan, and F. Capasso, "Whispering-gallery mode resonators for highly unidirectional laser action," *PNAS* **107**, p. 22407, 2010.
- [34] M. O. Scully, "Collimated unidirectional laser beams from notched elliptical resonators," *PNAS* **107**, p. 22367, 2010.
- [35] J. Y. Lee, B. H. Hong, W. Y. Kim, S. K. Min, Y. Kim, M. V. Jouravlev, R. Bose, K. S. Kim, I. Hwang, L. J. Kaufman, C. W. Wong, P. Kim, and K. S. Kim, "Near-field focusing and magnification through self-assembled nanoscale spherical lenses," *Nature* **460**, p. 498, 2009.
- [36] Z. Wang, W. Guo, L. Li, B. Luk'yanchuk, A. Khan, Z. Liu, Z. Chen, and M. Hong, "Optical virtual imaging at 50 nm lateral resolution with a white-light nanoscope," *Nat. Comm.* **2**, p. 1, 2011.
- [37] L. Gabrielli and M. Lipson, "Integrated luneburg lens via ultra-strong index gradient on silicon," *Opt. Expr.* **19**, p. 20122, 2011.
- [38] A. Falco, S. Kehr, and U. Leonhardt, "Luneburg lens in silicon photonics," *Opt. Expr.* **19**, p. 5156, 2011.

- [39] D. Gerard, J. Wenger, A. Devilez, D. Gachet, B. Stout, N. Bonod, E. Popov, and H. Rigneault, "Strong electromagnetic confinement near dielectric microspheres to enhance single-molecule fluorescence," *Opt. Expr.* **16**, p. 15297, 2008.
- [40] J. Schwartz, S. Stavrakis, and S. Quake, "Colloidal lenses allow high-temperature single-molecule imaging and improve fluorophore photostability," *Nat Nanotechnol.* **5**, p. 127, 2010.
- [41] L. Robledo, L. Childress, H. Bernien, B. Hensen, P. F. A. Alkemade, and R. Hanson, "High-fidelity projective read-out of a solid-state spin quantum register," *Nature* **477**, p. 574, 2011.
- [42] P. Siyushev, F. Kaiser, V. Jacques, I. Gerhardt, S. Bischof, H. Fedder, J. Dodson, M. Markham, D. Twitchen, F. Jelezko, and J. Wrachtrup, "Monolithic diamond optics for single photon detection," *Appl. Phys. Lett.* **97**, p. 241902, 2010.
- [43] H. Chew, "Transition rates of atoms near spherical surfaces," *J. Chem. Phys.* **87**, p. 1355, 1987.
- [44] V. Klimov, *Nanoplasmonics*, Pan Stanford Publishing, 2011.
- [45] B. Rolly, B. Stout, S. Bidault, and N. Bonod *Opt. Lett.* **36**, p. 3368, 2011.
- [46] T. Pakizeh and M. Kall, "Unidirectional ultracompact optical nanoantennas," *Nano Lett.* **9**, p. 2343, 2009.
- [47] S. A. Lavasani and T. Pakizeh, "Color-switched directional ultracompact optical nanoantennas," *Opt. Lett.* **29**, p. 1361, 2012.
- [48] A. Alu and N. Engheta, "Enhanced directivity from subwavelength infrared/optical nano-antennas loaded with plasmonic materials or metamaterials," *IEEE Trans. on Antennas and Propagation* **55**, p. 3027, 2007.
- [49] Z. Liu, H. Lee, Y. Xiong, C. Sun, and X. Zhang, "Far-field optical hyperlens magnifying sub-diffraction-limited objects," *Science* **315**, p. 1686, 2007.
- [50] Z. Jacob, L. Alekseyev, and E. Narimanov, "Optical hyperlens: Far-field imaging beyond the diffraction limit," *Opt. Expr.* **14**, p. 8247, 2006.
- [51] D. Lu and Z. Liu, "Hyperlenses and metalenses for far-field super-resolution imaging," *Nat. Comm.* **3**, p. 1, 2012.